The Lithium–Lithium Hydride System

Ewald Veleckis,* Erven H. Van Deventer, and Milton Blander

Chemical Engineering Division, Argonne National Laboratory, Argonne, Illinois 60439 *(Received February 22, 1974; Revised Manuscript Received June 17, 1974)*

Publication costs assisted by Argonne National Laboratory

Equilibrium hydrogen pressures (P_{H_2}) of lithium–lithium hydride mixtures sealed in iron capsules were measured over the following temperature–pressure–composition ranges: 710–903°, 0.5–760 Torr, and 0.5–99 mol % LiH. The isotherms show the phase diagram to consist of two homogeneous terminal solutions separated by a miscibility gap whose boundaries range from 25.2 and 98.4 mol % LiH at 710° to 45.4 and 85.5 mol % LiH at 903°. The data were fitted by a consistent thermodynamic treatment using the Margules forms for the activity coefficients. For each homogeneous solution region, this treatment yielded analytical expressions for the chemical potentials and activity coefficients of each species. The data show strong positive deviations from ideality of the solute species, especially in the LiH-rich solutions, where they may be related to the associative tendency of the lithium atoms. For dilute solutions of LiH in lithium, the ratio $N_{LiH}/(P_{H_2})^{1/2} = K'$ is given by $K'(\text{atm}^{-1/2}) = \exp(-6.498 + 6182T^{-1})$, where N_{LiH} is the mol fraction of LiH and T is the Kelvin temperature. For dilute solutions of Li in liquid LiH, the distribution of lithium between the gas and the solution phases is heavily weighted in favor of the latter, reflecting strong interactions between Li atoms and liquid LiH. The standard free energy of formation of liquid LiH is given by $\Delta G_f°$ (kcal/mol) = $13.47 \times 10^{-3}T - 16.55$.

Introduction

In many respects alkali–alkali hydride systems resemble alkali–alkali halide systems, which are much studied examples of metal–salt interactions.[1] Experimentally, the hydride systems offer an advantage in that one may obtain their thermodynamic properties by measuring equilibrium hydrogen pressures through membranes that are permeable to hydrogen only. A study of the Li–LiH system is particularly attractive because of the simplicity of the electronic structures of Li^+ and H^- ions, because most of the important features of its phase diagram lie in easily accessible ranges, and because studies of isotopic substitution of both lithium and hydrogen are feasible. In addition to this fundamental interest, the solution properties of Li–LiH, Li–LiD, and Li–LiT systems are important to the controlled thermonuclear research (CTR) program in which liquid lithium is a prime candidate for use as the breeder blanket fluid in fusion reactors.

The existing phase diagram and thermodynamic information on Li–LiH, Li–LiD, and Li–LiT systems has been reviewed by Messer.[2] For the Li–LiH system, Hill[3] obtained a single P_{H_2} *vs.* N_{LiH} isotherm at 700°, Perlow[4] extended this work by obtaining isothermal data at 770 and 825°, and Heumann and Salmon[5] remeasured the 700° isotherm. The solid LiH–liquid Li equilibrium was studied by Messer, *et al.*,[6] by the method of thermal analysis. From graphical representations[2] of the combined P_{H_2} *vs.* N_{LiH} data, it is apparent that the scatter in the data and an insufficient number of isotherms make it difficult to extract meaningful thermodynamic information, particularly in the dilute solution regions, where the disagreements result in crossing isotherms which also fail to pass through the origin. The same difficulties are found in the Li–LiD and Li–LiT systems, which were also briefly examined by Heumann and Salmon.[5]

Because of these shortcomings, we are conducting experimental studies to remeasure with improved precision the chemical activities and phase equilibria in the condensed systems Li–LiH, Li–LiD, and Li–LiT. The results obtained for the Li–LiH system are presented here.

Experimental Section

Apparatus. The experiments were carried out in a modified Sieverts' apparatus (shown in Figure 1) which consisted of three main sections designed for (a) gas purification, (b) gas metering, and (c) equilibration of the gas with an encapsulated Li–LiH melt.

In the first section, gases were purified by passing them through appropriate getters: liquid-nitrogen-cooled silica-gel for helium (the calibrating gas), and a hot titanium metal sponge for hydrogen. The titanium sponge, in conjunction with a 1-l. bulb, also served as a reservoir for large amounts of pure hydrogen needed for the experiments. A mercury bubbler protected against overpressure resulting from accidental overheating of the H_2-saturated sponge.

The gas metering section consisted of a water-thermostated (35°) bulb having a calibrated volume (~500 cm^3) between mark a and the three-way stopcock S, a mercury leveling bulb, and three pressure gauges in the ranges 0–20 (±0.05), 0–200 (±0.1), and 0–800 (±0.2) Torr for determining gas pressures in the calibrated bulb. The gauges were frequently calibrated *vs.* a mercury manometer.

The equilibration section, which extends from mark b to the sample volume, was comprised of (1) a double-walled fused-silica tube which contained the sample, (2) a partially thermostated manifold, and (3) three low-volume, high-precision gauges calibrated to within 0.05 Torr. Double-walled construction of the reaction tube was necessary because hydrogen has an appreciable permeability through fused silica at higher temperatures. [The permeation loss of hydrogen from a single-walled fused-silica tube was found to be high enough (0.5 standard cm^3/hr atm at 815°) to cause substantial errors in the data.] Hydrogen losses were minimized by automatically controlling, *via* a capaci-

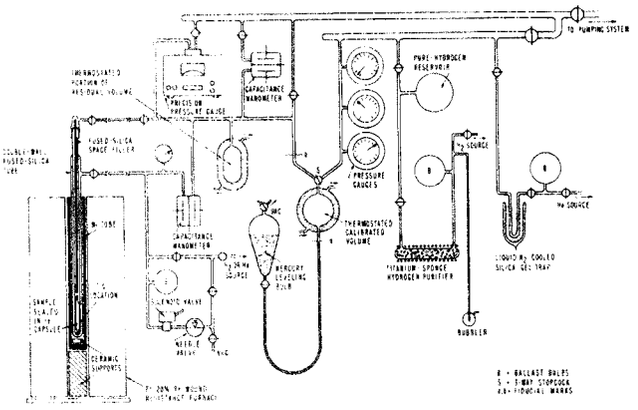

Figure 1. Apparatus for studying the Li–LiH system.

tance manometer, the hydrogen pressure in the annular space of the double-walled tube at the same value as that of the inner chamber.

The ambient temperature of the residual gases in the equilibration section was maintained uniform by (a) insulating the glass parts in the immediate vicinity of the furnace and (b) thermostating (at 35°) a major portion of the residual volume. A fused-silica rod space filler was placed inside the fused-silica tube to reduce the hot portion of the residual volume and to limit convection currents.

The sample was heated by a Pt–20% Rh-wound, single-zone Marshall tubular furnace (1.5-in. i.d., 20-in. long) in conjunction with a West SCR stepless temperature controller. The controller maintained temperatures constant to within 1° for periods greater than 1 hr. Temperatures were measured with three Pt—Pt–10% Rh thermocouples placed radially at 120° angles in the annular space of the tube at the sample level. The thermocouples were calibrated *in situ* against a standard thermocouple which was placed in an unsealed iron capsule filled with lead metal substituting for lithium.

Containment of Lithium. Because of the high volatility and reactivity of alkali metals, there are problems associated with open-cell techniques.[7] Consequently, in this study, lithium was contained in closed capsules (2.25-in. long, 0.5-in. diameter cylinders with 0.015-in. wall) made of Armco iron tubing. Iron was selected on the basis of its corrosion resistance toward lithium,[8] relatively high hydrogen permeability,[9] and low hydrogen solubility.[10] To facilitate the loading of lithium, the ends of the capsules were made in the shape of a funnel with the stems facing outward. Before loading, the capsules were heated in hydrogen and then degassed at 850–900°.

The capsules were filled with lithium according to the following procedure. A glass stopcock was attached, *via* a glass-to-metal seal, to the top funnel stem and a 5-μm porosity stainless-steel filter was attached to the bottom stem of a capsule. The assembly was placed in a high-purity helium atmosphere glove box (~1 ppm of nitrogen and oxygen) and the bottom half of the capsule was filled by (a) immersion of the filter end in a pot of molten lithium and (b) application of gentle suction through the stopcock. The capsule was then cooled to room temperature and the bottom funnel stem was closed by a heli-arc weld. After removal from the glove box, the capsule was evacuated to 10^{-6} Torr and, after flattening part of the top funnel stem, the glass portion was sealed with a flame. The capsule was then sealed and cut *in vacuo* at the flattened portion by electron-beam welding.

Each loaded capsule was tested for leaks and degassed by heating at ~900° *in vacuo*. (The capsule used for the measurements at 710° was degassed at ~700°). Care was taken not to exceed the α–γ transformation point of iron (910°). New capsules required 2–3 days for degassing; used capsules, already containing hydrided lithium, required about 2 weeks.

The evacuated space of the capsule (2–4 cm^3) is expected to be filled with lithium vapor which may react with hydrogen to form gaseous LiH.[11] Below the monotectic temperature (685°), condensation of solid hydride on the capsule walls could inhibit hydrogen diffusion; above this temperature, however, LiH is liquid and should be adequately drained from the capsule walls. Accordingly, all the experiments but one were conducted at temperatures above the monotectic.

Procedure. For each hydridation experiment, a new Armco iron capsule containing approximately 2 g of pure, degassed lithium was placed in the double-walled tube. The tube was connected to the apparatus, evacuated, and heated to the temperature of the experiment. The effective volume of the equilibration section of the apparatus was then determined by filling it several times with known amounts of helium and measuring the pressure each time. Helium was selected as the calibrating gas because its thermal conductivity is most nearly equal to that of hydrogen. After the calibration, the helium was pumped off.

Hydrogen was then added to the sample in 20 to 30 portions. The size of these portions was varied in such a way as to aid in the delineation of an isotherm. Thus, at the very low and the very high hydrogen concentrations, where the isotherm is steep, small additions (2–6 mmol of H_2) were used, whereas, in the extensive plateau portions, the additions were quite large (20–25 mmol of H_2). For each addition, the amount of hydrogen was measured in the calibrated bulb. The contents of the bulb were then quantitatively transferred into the equilibration section by flooding the bulb with mercury up to the mark b. Successive portions of hydrogen were added using this procedure until the equilibrium hydrogen pressure approached 1 atm. Equilibrium was considered established when the recorded pressure *vs.* time charts showed no further pressure changes (±0.01 Torr) for at least 6 hr. The validity of this criterion for equilibrium was confirmed by our observation of a correspondence between the observed kinetics of hydrogen uptake and equations derived from a diffusion model. According to Heumann and Salmon,[5] the rate of hydrogen uptake by lithium sealed in iron capsules (same wall thickness as in our work) was very nearly equal to that expected for hydrogen diffusion through iron. They allowed 8–12 hr for each equilibration. The amount of lithium used in the present work was ~50 times larger and the time required to reach equilibrium was 12–48 hr, depending on the quantity of hydrogen added, on the temperature, and on the equilibrium hydrogen pressure.

During the course of experiments, several desorption measurements were carried out as a test of thermodynamic reversibility. This was accomplished by removing a measured amount of hydrogen (by Toepler pumping) and measuring the pressure after the reestablishment of equilibrium.

The concentration of hydrogen in lithium resulting from each hydrogen addition was calculated from the weight of lithium and from the total hydrogen added which was corrected for the amounts of hydrogen remaining in the resid-

ual volume, in the vapor space inside the capsule, and dissolved in iron. The latter two amounts combined were less than 0.04% of the total hydrogen content. The fraction of hydrogen remaining in the residual volume ranged from ~6% at 10 Torr to ~15% at 760 Torr.

Materials. Lithium metal ingots, packed under argon and having a stated purity of 99.98%, were purchased from the Foote Mineral Co. The major metallic impurities were found to be sodium (79 ppm) and potassium (35 ppm). The measured $^6Li/^7Li$ atom ratio was 0.0815 ± 0.0007, in good agreement with the accepted value for natural lithium.

Analysis of Data

If we assume that hydrogen in the condensed phase is in the form of a hydride, then the equilibrium reaction between gaseous hydrogen and liquid lithium may be written as

$$\frac{1}{2}H_2(g, T, P_{H_2}) + Li(soln, T, P_{H_2}) \rightleftharpoons LiH(soln, T, P_{H_2}) \quad (1)$$

The equilibrium constant, K, for this reaction is given by

$$K = N_2\gamma_2/N_1\gamma_1(P_{H_2})^{1/2} \quad (2)$$

where the subscripts 1 and 2 refer to Li and LiH, respectively, the N's are the mole fractions of the components in the condensed phase, the γ's are the corresponding activity coefficients, P_{H_2} is the equilibrium hydrogen pressure in atmospheres, and T is the Kelvin temperature. Equation 2 can be rewritten in the form

$$\ln [(P_{H_2})^{1/2} N_1/N_2] = -\ln K + \ln (\gamma_2/\gamma_1) \quad (3)$$

According to Margules, the activity coefficients of the components in a binary solution may be represented by a power series in N.[12] When the series are truncated at their cubic terms, the activity coefficients are consistently given by

$$\ln\gamma_1 = \alpha N_2^2 + \beta N_2^3 \quad (4)$$

and

$$\ln \gamma_2 = \left(\alpha + \frac{3}{2}\beta\right) N_1^2 - \beta N_1^3 \quad (5)$$

Substitution of eq 4 and 5 into eq 3 yields a second-order power series for $\ln [(P_{H_2})^{1/2}N_1/N_2]$ *vs.* N_2, *i.e.*

$$\ln [(P_{H_2})^{1/2} N_1/N_2] =$$

$$-\ln K + \alpha(1 - 2N_2) + (1/2)\beta(1 - 3N_2^2) \quad (6)$$

At the extreme limits of the composition range, $N_2 \rightarrow 0$ and $N_2 \rightarrow 1$, eq 6 becomes

$$\lim_{N_2 \to 0} \ln [(P_{H_2})^{1/2}/N_2] = -\ln K + \alpha + (1/2)\beta \quad (7)$$

and

$$\lim_{N_2 \to 1} \ln [(P_{H_2})^{1/2} N_1] = -\ln K - \alpha - \beta \quad (8)$$

The data from the hydridation experiments consist of sets of isothermal pressure–composition values.[13] A convenient method of graphical representation of these data is to project each set of isothermal values on the square root of hydrogen pressure *vs.* composition plane. Six isotherms (at 710, 759, 803, 847, 878, and 903°) were obtained for the system Li–LiH and are exhibited in this manner in Figure 2.

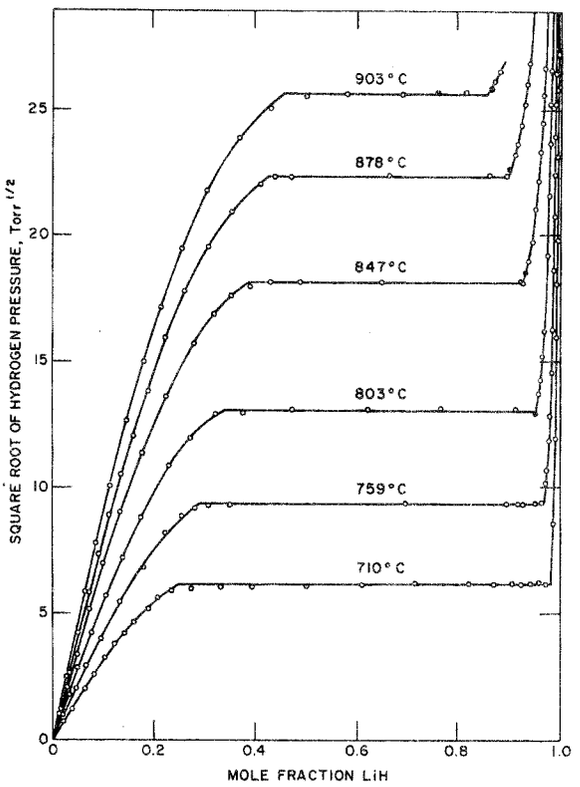

Figure 2. Projection of the hydridation data on the square root of hydrogen pressure *vs.* composition plane for the system Li–LiH. Solid points indicate desorption measurements.

The pressure–composition data obtained from the hydridation experiments were corrected for (1) the average temperature of the isotherm to which the data belonged, (2) the initial hydrogen concentration in lithium, and (3) the stoichiometry of LiH. The nature of these corrections is described below.

(1) Because of the temperature fluctuations in the furnace, each datum point on an isotherm was recorded at a slightly different temperature (WITHIN ±[°(/ Therefore, each pressure reading was corrected to the average temperature for that isotherm. The corrections were based on the temperature coefficients calculated, as a function of composition, from all six isotherms.

(2) According to eq 7, plots of $\ln [(P_{H_2})^{1/2}N_1/N_2]$ *vs.* N_2 should intersect the ordinate at finite values. Figure 3a shows such plots for the first rising portions of the isotherms. In all cases, as $N_2 \rightarrow 0$, the curves tended to bend sharply upward. The most plausible explanation of this behavior is that, due to incomplete degassing, some residual hydrogen is retained in the encapsulated lithium at the start of the experiments. This assumption is supported by the fact that the effect was larger for the first isotherm (at 710°) for which the lithium sample was degassed less completely, at a lower temperature (700°), and for a shorter time.

The data were corrected by applying increments, ϵ, to the N_2's in eq 6. The increments represent the estimated initial mole fraction of LiH in lithium. For each isotherm, the value of ϵ was selected such that a least-squares fit of $\ln [(P_{H_2})^{1/2}(1 - N_2 - \epsilon)/(N_2 + \epsilon)]$ *vs.* $(N_2 + \epsilon)$ showed a minimum in the sum of the squared residuals. The resulting

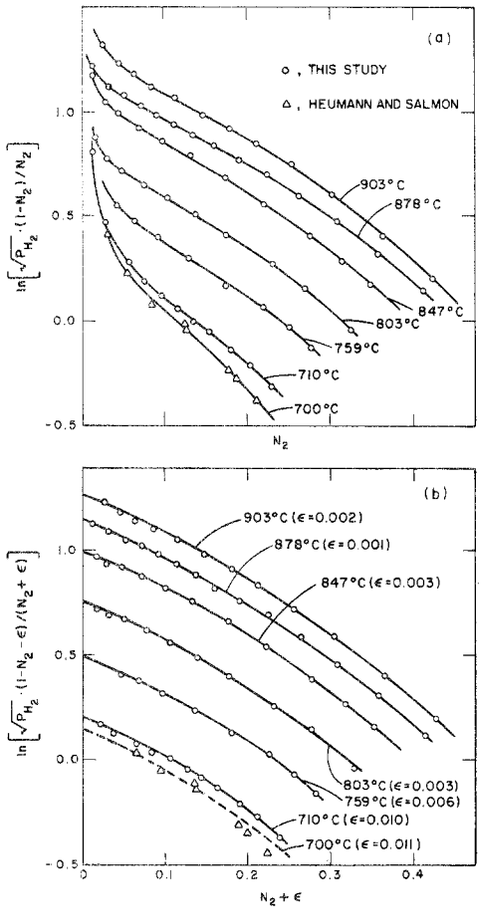

Figure 3. Effect of residual hydrogen concentration, ϵ, on the shape of isotherms in the dilute region of the Li–LiH system: (a) original data, (b) data corrected for ϵ.

curves and the corresponding ϵ values are shown in Figure 3b.

This corrective procedure was also applied to the hydridation data (at 700°) of Heumann and Salmon[5] which show a similar upward trend in the dilute region (Figure 3a). After the correction (ϵ = 0.011), their data agree reasonably with the values extrapolated from ours (dashed curve in Figure 3b).

One may speculate about the sources of the residual hydrogen. One possibility is the retention of hydrogen by the lithium during its manufacture. This could not be confirmed because of the difficulties associated with the vacuum fusion analysis of liquid lithium. Another source of hydrogen could be the presence of adsorbed water on the surfaces in the vicinity of the iron capsule. Calculations show that owing to the equilibria $Fe + H_2O \rightleftarrows FeO + H_2$ and $3Fe + 4H_2O \rightleftarrows Fe_3O_4 + 4H_2$, the partial pressures of water necessary to produce the requisite residual hydrogen concentration are, on the average, only 6×10^{-4} Torr (ϵ = 0.001) and 6×10^{-2} Torr (ϵ = 0.01) at 700° and 8×10^{-3} Torr (ϵ = 0.001) and 8×10^{-1} Torr (ϵ = 0.01) at 900°. These results also stress the importance of prolonged high-temperature degassing of encapsulated lithium prior to an experiment.

(3) When the data of the second rising portions of the isotherms are plotted as $1/(P_{H_2})^{1/2}$ *vs.* N_1, the extrapolated $[1/(P_{H_2})^{1/2} \rightarrow 0]$ least-squared curves did not intersect the abscissa at exactly $N_1^0 = 0$, as required by eq 8, but rather at $N_1^0 = -0.013$ (at 710°), −0.007 (759°), −0.016 (803°), −0.008 (847°), −0.014 (878°), and −0.007 (903°). Because in the case of lithium a stoichiometric hydride is expected, the slight bias in N_1^0 was attributed to errors accumulated in numerous hydrogen additions during the experiment. A correction was applied by multiplying all N_2's of an isothermal data set by its respective normalization factor, $1/(1 - N_1^0)$. (If LiH was found to be nonstoichiometric, it would be simple to adjust our data to take this finding into account.)

Results

Each of the isotherms comprises two rising portions that are separated by a horizontal line. The composition ranges of the first and second rising portions correspond to homogeneous phases; the constant-pressure plateau defines the two-phase coexistence region. This shape of the isotherms supports the expected[1] analogy between the Li–LiH system and the alkali–alkali halide systems. The temperature–composition phase diagrams of the latter systems[14] consist of a monotectic horizontal above which there is a closed region of coexistence of two liquids and below which a solid salt containing very small amounts of metal is in equilibrium with a solution of salt in the liquid metal. A monotectic horizontal for the Li–LiH system has been reported[6] at 685 ± 1°.

The desorption data are also shown in Figure 2. No evidence of hysteresis was observed, thus confirming the reversibility of the hydrogen–lithium reactions. Because of the particular apparatus used, the hydrogen pressures were limited within the range 0.5–760 Torr. The error in the individual pressure measurements was estimated to be ±0.5%, resulting primarily from the fluctuations in the ambient temperature of the residual volume.

An attempt was made to determine an isotherm at 653°, *i.e.*, below the monotectic temperature. For the first rising portion of this isotherm, hydrogen absorption rates were similar to those observed at the higher temperatures; however, when the pressure plateau was approached, hydrogen uptake was slowed down to impractical levels, probably owing to a coating of solid LiH on the inside walls of the capsule. The experiment was discontinued and only an approximate value (15.5 ± 1.5 mol % LiH) could be estimated for the solubility of solid LiH in liquid lithium.

The miscibility gap data are presented in Table I. Items in Table I are discussed below.

Plateau Dissociation Pressures. A review of the literature data on the plateau pressures, P_{H_2}, for the Li–LiH system has been made elsewhere.[2] The results obtained in this study, combined with the six pieces of data reported by Heumann and Salmon[5] (at 728, 728.5, 756, 774, 785, and 804°), may be represented by

$$\ln P_{H_2}(\text{Torr}) = 21.128 - 17,186T^{-1} \qquad (9)$$

with an uncertainty of only 1.5% (at the 95% confidence level) in the predicted value of P_{H_2}. [The seventh datum point (at 700°) of Heumann and Salmon fell outside the error band and was omitted from the least-squares analysis.] Statistical F tests showed that both sets of data originated from the same population. The data of older work[2] appear to be less reliable and are excluded.

Miscibility Gap Limits. The lower limit, N_2'(satd), represents the solubility of LiH in liquid lithium; the upper limit, N_2''(satd), that of lithium in liquid LiH. The logarithms of both limits are shown as functions of temperature in Figure 4; they may be represented by

TABLE I: Miscibility Gap Data of the System Li–LiH

T, °C	Plateau pressure,[a] Torr	Miscibility gap limits[a] N_2'(satd)	N_2''(satd)	Activity coefficients[b] γ_1'(satd)	γ_2'(satd)	γ_1''(satd)	γ_2''(satd)
710	38.5	0.252	0.984	1.084	4.02	49.7	1.002
759	88.3	0.285	0.971	1.122	3.35	28.6	1.006
803	171.4	0.332	0.957	1.169	2.87	17.6	1.013
847	329.2	0.386	0.923	1.230	2.47	10.1	1.032
878	500.2	0.418	0.888	1.283	2.23	6.80	1.059
903	658.8	0.454	0.855	1.333	2.06	5.05	1.090

[a] Observed data from which eq 9–11 were derived. [b] Calculated from eq 19–22 with N_2(satd) values derived from eq 10 and 11.

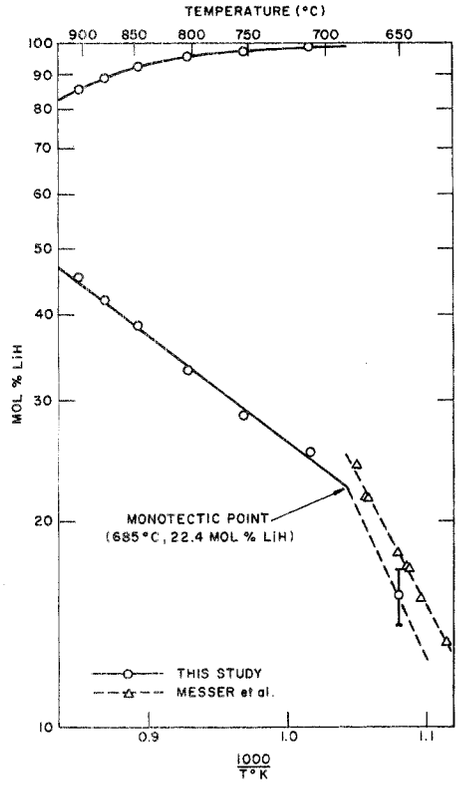

Figure 4. Temperature dependence of the miscibility gap boundaries for the Li–LiH system.

$$\ln N_2'(\text{satd}) = 2.235 - 3,576T^{-1} \quad (10)$$

and

$$\ln N_2''(\text{satd}) = -36.5585 + 1.10246 \times 10^5 T^{-1} - 1.11116 \times 10^8 T^{-2} + 3.74082 \times 10^{10} T^{-3} \quad (11)$$

The errors estimated for N_2'(satd) and N_2''(satd) were ±0.01 and ±0.005, respectively.

An extrapolation was made into the region below the monotectic temperature (685°) by connecting the monotectic point (22.4 mol % LiH according to eq 10) with our approximate single solubility value for the solid LiH. This value, together with the freezing points of mixtures of LiH and lithium, measured in the range 624–679° by thermal analysis,[6] is also shown in Figure 4. There is an apparent discrepancy between the two sets of data. Because of the relative steepness of the freezing-point curve, the thermal values may not be as reliable as desired. Need for further work in this area is indicated.

Discussion

Because of the width and the asymmetry of the miscibility gap in the Li–LiH system, it is difficult to find continuous functions of the activity coefficients that would simultaneously satisfy the data for both terminal solutions. As an alternative, we chose to obtain activity coefficient expressions separately for each terminal solution.

Two conditions must be met in this data treatment: (1) the same equilibrium constant must govern both regions, and (2) the chemical activities of a component must be the same on both sides of the miscibility gap, *i.e.*, $N_1'(\text{satd})\gamma_1'(\text{satd}) = N_1''(\text{satd})\gamma_1''(\text{satd})$ and $N_2'(\text{satd})\gamma_2'(\text{satd}) = N_2''(\text{satd})\gamma_2''(\text{satd})$, where the single and double prime superscripts refer to the first and the second terminal solutions, the designation (satd) indicates the value at the miscibility gap boundary, and standard states of Li and LiH are the pure liquid phases. In spite of the relatively small scatter in the data, it was not possible to meet these conditions exactly at each datum point. Instead, a statistical treatment was sought.

The equilibrium constant, K, was regarded as an adjustable parameter, subject to the constraint

$$K = \frac{N_2''(\text{satd})\gamma_2''(\text{satd})}{N_1'(\text{satd})\gamma_1'(\text{satd})[P_{H_2}(\text{plateau})]^{1/2}} \quad (12)$$

which resulted from the combination of eq 2 and the above equalities. In eq 12 the γ's are subscripted to refer to those solution components which are at higher concentrations at the miscibility gap boundaries. This choice of γ's is convenient because their values are never far removed from unity and can be more precisely determined from the data (see, *e.g.*, Table I). Next, eq 6 was transformed into two linear equations, one for each terminal solution

$$Z_{ij}' = A_1'Y_{ij}' + B_1'X_i'Y_{ij}' + A_2'W_{ij}' + B_2'X_i'W_{ij}' \quad (13)$$

and

$$Z_{ij}'' = A_1''Y_{ij}'' + B_1''X_i''Y_{ij}'' + A_2''W_{ij}'' + B_2''X_i''W_{ij}'' \quad (14)$$

where the indices i and j refer to temperature and concentration, respectively, and the symbols are defined as follows: $Z_{ij} = \ln [K_i(P_i)^{1/2}(N_1/N_2)_{ij}]$, $Y_{ij} = (1 - 2N_2)_{ij}$, $W_{ij} = (1 - 3N_2^2)_{ij}$, $X_i = (1/T)_i$, $\alpha_i' = A_1' + B_1'X_i$, $\beta_i' = A_2' + B_2'X_i$, $\alpha_i'' = A_1'' + B_1''X_i$, $\beta_i'' = A_2'' + B_2''X_i$.

With the use of an initial estimated value of the equilibrium constant, the eight A and B parameters in eq 13 and 14 were evaluated by the method of least squares from 118 pieces of observed pressure–temperature–composition data of the terminal solution regions. Improved values of K were then calculated from the resulting A and B parameters using eq 12. Generally, K converged after five iterations.

The final ln K *vs.* $1/T$ points, when plotted, exhibited only a very slight deviation from linearity and therefore

could be represented by the equation

$$\ln K\ (\mathrm{atm}^{-1/2}) = -6.780 + 8328T^{-1} \quad (15)$$

with an error of only 0.5% (95% confidence level) in the mean value of K. The corresponding expression for the standard free energy of formation of liquid LiH, $\Delta G_f^\circ = [\mu_{LiH}^0(l,T,P_{H_2}) - \mu_{Li}^0(l,T,P_{H_2}) - \frac{1}{2}\mu_{H_2}^0(g,T,1\ \mathrm{atm})]$, is given by

$$\Delta G_f^\circ\ (\mathrm{kcal/mol}) = 13.47(\pm 0.17) \times 10^{-3}T - 16.55(\pm 0.18) \quad (16)$$

ΔG_f° values calculated from eq 16 (*e.g.*, −3.07 kcal/mol at 1000°K, −0.38 at 1200°K) are slightly lower than the independently determined values listed in the JANAF tables[15] (−2.859 at 1000°K, −0.288 at 1200°K).

Final values of the parameters in eq 13 and 14, calculated with K's represented by eq 15, are $A_1' = -0.2295$, $A_2' = -0.1039$, $A_1'' = 25.127$, $A_2'' = -29.669$, $B_1' = 986.5$°K, $B_2' = 2{,}308$°K, $B_1'' = -30{,}699$°K, $B_2'' = 39{,}285$°K.

Using these parameters one can numerically express the change in the chemical potential of the reaction in eq 1 as a function of temperature and concentration. Since this change in the chemical potential is defined by $[\mu_{LiH}(\mathrm{soln}, T,P_{H_2}) - \mu_{Li}(\mathrm{soln},T,P_{H_2}) - \frac{1}{2}\mu_{H_2}^0\ (g,T,1\ \mathrm{atm})] = RT \ln (P_{H_2})^{1/2}$, we have from eq 6, for the first terminal solution

$$\ln (P_{H_2})^{1/2} = \ln (N_2/N_1) + 6.498 + 0.4589N_2 + 0.1558N_2^2 - (1/T)(6182 + 1973N_2 + 3462N_2^2) \quad (17)$$

and, for the second terminal solution

$$\ln (P_{H_2})^{1/2} = \ln (N_2/N_1) + 11.322 - 38.753N_1 + 44.504N_1^2 - (1/T)(16{,}914 - 56{,}457N_1 + 58{,}928N_1^2) \quad (18)$$

where P_{H_2} is the equilibrium hydrogen pressure in atmospheres.

Equations 17 and 18 can be used to construct any isotherm within the temperature range of this study. For that purpose, the plateau pressures and the miscibility gap boundaries are given by eq 9–11. When the isotherms are calculated at the experimental temperatures of this study and are then superimposed on the data points (in a plot similar to that of Figure 2), the agreement is excellent at 710, 759, 803, and 847°, whereas at 878 and 903°, some deviations occur in the plateau region, caused mainly by a larger scatter in the plateau pressure values at these temperatures. The largest deviations occur at 903°, near the lower boundary of the miscibility gap, but even here they amount to less than 3%. Such a deviation would correspond to an uncertainty in temperature of less than 2°.

Equations 17 and 18 were also used to obtain the temperature and composition of the consolute point by equating to zero the first derivatives with respect to N and solving the resulting equations. The calculations yielded (to five significant figures) 1000° and 60.0 mol % LiH. The former value is in good agreement with the consolute temperature reported by Heumann and Salmon (997°).[5]

The activity coefficients of Li and LiH in the first (γ_1', γ_2') and in the second (γ_1'', γ_2'') terminal solutions were obtained from the A and B parameters and from eq 4 and 5. Thus

$$\ln \gamma_1'/N_2^2 = (-0.2295 - 0.1039N_2) + (1/T)(986.5 + 2308N_2) \quad (19)$$

$$\ln \gamma_2'/N_1^2 = (-0.3853 + 0.1039N_1) + (1/T)(4448 - 2308N_1) \quad (20)$$

$$\ln \gamma_1''/N_2^2 = (25.127 - 29.669N_2) - (1/T)(30{,}699 - 39{,}285N_2) \quad (21)$$

$$\ln \gamma_2''/N_1^2 = (-19.377 + 29.669N_1) + (1/T)(28{,}228 - 39{,}285N_1) \quad (22)$$

Activity coefficients, calculated from eq 19–22 for concentrations corresponding to the miscibility gap boundaries, are listed in Table I. Their values indicate that the positive deviations from ideality in the LiH-rich solutions are much larger than those in the Li-rich solutions, as would be expected from the direction of the asymmetry of the miscibility gap. It is also interesting to note that according to eq 20 the excess entropy, $\Delta\bar{S}^E = -R[\partial(T \ln \gamma)/\partial T]$, of LiH in the Li-rich solutions is small (0.3–0.6 eu at 800°). Although this is common in binary molten-salt solutions,[16] the result is surprising because of the relatively large differences in bonding characteristics between Li and LiH. In contrast, the excess entropy (calculated from eq 21) of Li in the LiH-rich solutions (4–9 eu at 800°) appears to be unusually large. This may be related to an apparent tendency for the alkali metals, especially lithium, to associate in solutions.[14]

Additional important thermodynamic information that has bearing on the fundamental interactions between Li and LiH in solutions can be obtained by considering two limiting cases.

Dilute Solutions of LiH in Liquid Lithium. From the condition $N_2 \to 0$, it follows that $N_1\gamma_1 \to 1$, $\gamma_2 \to \gamma_2^*$, and eq 2 reduces to

$$K = K'\gamma_2^* \quad (23)$$

Here, γ_2^* is the activity coefficient of LiH at infinite dilution. It corresponds to the change in state $RT \ln \gamma_{LiH}^* = [\mu_{LiH}^*(T,P_{H_2}) - \mu_{LiH}^0(l,T,P_{H_2})]$ where $\mu_{LiH}^*(T,P_{H_2})$ is the chemical potential of LiH in a standard state defined in terms of an infinite dilution of LiH in Li, and $\mu_{LiH}^\circ(l, T,P_{H_2})$ is the chemical potential of pure liquid LiH. $K' = N_2/(P_{H_2})^{1/2}$ is a temperature-dependent constant[17] corresponding to the change in state $RT \ln K' = -[\mu_{LiH}^*(T,P_{H_2}) - \mu_{Li}^0(l,T,P_{H_2}) - \frac{1}{2}\mu_{H_2}^0(g,T,1\ \mathrm{atm})]$.

Numerically, γ_{LiH}^* may be evaluated[18] by applying the condition $N_1 = 1$ to eq 20. K' is then calculated according to eq 23. Thus

$$\ln K'\ (\mathrm{atm}^{-1/2}) = -6.498 + 6182T^{-1} \quad (24)$$

The knowledge of P–T–C relations in dilute solutions (<1 ppm) of hydrogen isotopes in liquid lithium is important in the CTR program. For dilute solutions, the hydrogen pressures calculated from eq 24 very well approximate those obtained from the more complex eq 17. For example, in the temperature range of this study, the difference in the hydrogen pressures calculated from the two equations is <1% for $N_{LiH} = 0.01$ and <0.1% for $N_{LiH} = 0.001$.

Dilute Solutions of Li in Liquid LiH. For the second terminal solution region, as $N_1 \to 0$, $N_2\gamma_2 \to 1$, and $\gamma_1 \to \gamma_1^*$, eq 2 becomes

$$K = K''/\gamma_1^* \quad (25)$$

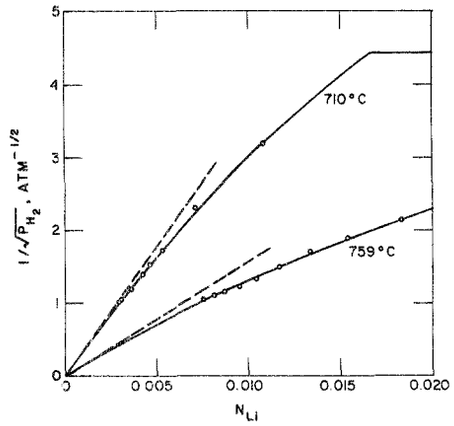

Figure 5. Portions of two lowest temperature isotherms showing the approach to a limiting law in the Li-rich solutions: (O) experimental points, (——) isotherms calculated from eq 18, (– – –) limiting slopes calculated from eq 26.

where γ_1^* is the activity coefficient of lithium at infinite dilution defining the change in state $RT \ln \gamma_1^* = [\mu_{Li}^*(T,P_{H_2}) - \mu_{Li}^0(l,T,P_{H_2})]$, and $K'' = 1/[N_1(P_{H_2})^{1/2}]$ is a constant analogous to K'. In terms of the chemical potentials, K'' corresponds to $RT \ln K'' = -[\mu_{LiH}^0(l,T,P_{H_2}) - \mu_{Li}^*(T,P_{H_2}) - \frac{1}{2}\mu_{H_2}^0(g,T,1\text{ atm})]$. When the values of γ_1^* are evaluated[18] from eq 21 (at $N_2 = 1$), those of K'' may be obtained from eq 25. Thus

$$\ln K'' \text{ (atm}^{-1/2}) = -11.322 + 16,908T^{-1} \quad (26)$$

According to the definition of K'', a plot of $1/(P_{H_2})^{1/2}$ *vs.* N_1 should approach linearity, as $N_1 \to 0$. In Figure 5 we present such plots at the two lowest temperatures of this study, 710 and 759°. It is evident that the experimental points support the limiting linearity requirements; however, because of the data normalization discussed above, a positive proof must await more detailed data in this terminal region.

Further useful thermodynamic information for solutions in this region is obtained by considering the following equilibrium

$$\text{Li}(g, T, P_{Li}) \rightleftharpoons \text{Li(soln}, T, P_{Li}) \quad (27)$$

As $N_{Li} \to 1$ and $\gamma_{Li} \to 1$, the equilibrium constant and the corresponding change in the chemical potentials are given by

$$K_h = \frac{N_{Li}}{P_{Li}} = \exp\left[-\frac{\mu_{Li}^*(T,P_{Li}) - \mu_{Li}^0(g,T,1\text{ atm})}{RT}\right] \quad (28)$$

where P_{Li} is the partial pressure of lithium in the vapor phase, K_h is Henry's law constant, $\mu_{Li}^*(T,P_{Li})$ is the standard chemical potential of lithium defined at infinite dilution, and $\mu_{Li}^0(g,T,1\text{ atm})$ is the standard chemical potential of lithium vapor. No direct measurements for P_{Li} are available but, since $a_{Li} = N_{Li}\gamma_{Li} = P_{Li}/P_{Li}^0$, it can be replaced by the product $P_{Li}^0 N_{Li}\gamma_{Li}$. Thus

$$\ln K_h \text{ (atm}^{-1}) = -\ln (P_{Li}^0\gamma_{Li}^*) = -6.994 + 9986T^{-1} \quad (29)$$

where P_{Li}^0, the vapor pressure of pure liquid lithium, is given[19] by $\ln P_{Li}^0 \text{ (atm)} = 11.536 - 18,572T^{-1}$, and γ_{Li}^* is obtained from eq 21 (with $N_2 = 1$).

A more useful way of describing the equilibrium reaction in eq 27 is in terms of the Ostwald coefficient, λ, defined by

$$\lambda = (C_{soln}/C_g) = \exp\left[-\frac{\mu_{Li}^*(T,P_{Li}) - \mu_{Li}^0(g,T,P_{Li} = R'Td_{LiH}/M_{LiH})}{RT}\right] \quad (30)$$

where C_{soln} and C_g are the concentrations (in mol/cm^3) of lithium in the solution and in the ideal vapor phase, respectively, $R' = 82.06$ cm^3 atm/deg mol is the gas constant, d_{LiH} is the density[20] of liquid LiH, and M_{LiH} is the molecular weight of LiH. The standard chemical potential $\mu_{Li}^0(g, T,P_{Li} = R'Td_{LiH}/M_{LiH})$ corresponds to 1 mol of ideal lithium vapor at temperature T and in a volume equal to the molar volume of solvent LiH. This standard state differs from $\mu_{Li}^0(g,T,1\text{ atm})$ in eq 28 in that it eliminates the physically unimportant contribution arising from differences in the molar volumes of the two phases. Thus, the quantity $RT \ln \lambda$ in eq 30 can be interpreted as the standard free energy of vaporization of lithium from the solution phase into the same volume of the vapor phase and is a direct measure of the interaction of Li atoms with molten LiH. The quantities K_h and λ are related by $\lambda = K_h R'Td_{LiH}/M_{LiH}$ and, according to eq 29

$$\ln \lambda = \ln (d_{LiH}T) - 4.659 + 9986T^{-1} \quad (31)$$

Topol[21] has estimated values of $RT \ln \lambda$ for 34 molten metal–metal chloride solutions at ~1000°K. For the alkali metal systems he obtained 20, 10, 11, and 10 kcal/mol for the Li–LiCl, Na–NaCl, K–KCl, and Rb–RbCl systems, respectively. From eq 31 for the Li–LiH system we obtain 23.1 kcal/mol, a value similar to Topol's estimate for Li–LiCl. The standard entropy and enthalpy of vaporization of lithium from LiH solutions, calculated at 1000°K by differentiating eq 31 with respect to temperature, are respectively −4.9 eu and 18.2 kcal/mol.

A large positive value of the free energy of vaporization indicates that the distribution of lithium between the gas and the molten hydride phase is heavily weighted in favor of the latter and reflects very strong interactions between lithium and LiH. This is in contrast to the solutions of noble gases in sodium[22] and in molten fluorides,[23] where the Ostwald coefficients are small ($\lambda \simeq 10^{-3}$) and therefore the distribution of the noble gas is strongly shifted in favor of the gas phase.

The results obtained in this study appear to be more precise than those of previous work. Several factors might have contributed to the improved precision: (a) the use of a larger quantity of lithium, (b) the absence of gases other than hydrogen in contact with lithium, (c) the prevention of hydrogen leakage from the reaction tube (double-walled construction), (d) the stabilization of hydrogen pressures by thermostating a major portion of the residual volume, (e) the thermostating of the calibrated volume for hydrogen metering, (f) the use of pure hydrogen generated by thermal decomposition of TiH_2, (g) the length of the equilibration times, and finally (h) the corrections for the initial concentration of hydrogen in the sample.

A similar investigation of the Li–LiD system is in progress.

Acknowledgments. We thank F. J. Karasek for manufacturing the Armco iron tubing and Dr. H. M. Feder, Dr. V. A. Maroni, and Professor S. E. Wood for helpful discus-

sions. This work was performed under the auspices of the U. S. Atomic Energy Commission.

Supplementary Material Available. Tabular results of the measurements will appear following these pages in the microfilm edition of this volume of the journal. Photocopies of the supplementary material from this paper only or microfiche (105 × 148 mm, 24× reduction, negatives) containing all of the supplementary material for the papers in this issue may be obtained from the Journals Department, American Chemical Society, 1155 16th St., N.W., Washington, D. C. 20036. Remit check or money order for $3.00 for photocopy or $2.00 for microfiche, referring to code number JPC-74-1933.

References and Notes

(1) W. M. Mueller, J. P. Blackledge, and G. G. Libowitz, "Metal Hydrides," Academic Press, New York, N. Y., 1968.
(2) C. E. Messer, "A Survey Report on Lithium Hydride," AEC Research and Development Report No. NYO-9470, 1960.
(3) L. O. Hill, Ph.D. Dissertation, University of Chicago, 1938.
(4) M. R. J. Perlow, Ph.D. Dissertation, University of Chicago, 1941.
(5) F. K. Heumann and O. N. Salmon, "The Lithium Hydride, Deuteride, and Tritide Systems," USAEC Report No. KAPL-1667, 1956.
(6) C. E. Messer, E. B. Damon, P. C. Maybury, J. Mellor, and R. A. Seales, *J. Phys. Chem.*, **62**, 220 (1958).
(7) S. A. Meacham, E. F. Hill, and A. A. Gordus, "The Solubility of Hydrogen in Liquid Sodium," Atomic Power Development Associates, Inc., Report No. APDA-241, 1970.
(8) M. F. Amateau, "The Effect of Molten Alkali Metals on Containment Metals and Alloys at High Temperatures," Defense Metal Information Center, Report No. DMIC-169, 1962.
(9) R. W. Webb, "Permeation of Hydrogen Through Metals," Atomics International, Report No. NAA-SR-10462, 1965.
(10) P. D. Blake, M. F. Jordan, and W. I. Pumphrey, *Iron Steel Inst., Spec. Rep.*, **73**, 76 (1962).
(11) H. R. Ihle and C. H. Wu, "Mass-Spectrometric Knudsen Effusion Measurements of Vapor Species in the System Lithium-Hydrogen," Report No. EUR-4938, p 89, from the 7th Symposium on Fusion Technology, Grenoble, France, Oct 1972.
(12) See, *e.g.*, J. H. Hildebrand and R. L. Scott, "The Solubility of Nonelectrolytes," 3rd ed, Reinhold, New York, N. Y., 1950, p 34.
(13) See paragraph at end of text regarding supplementary material.
(14) M. A. Bredig in "Molten Salt Chemistry," M. Blander, Ed., Interscience, New York, N. Y., 1964, p 386.
(15) "JANAF Thermochemical Tables," Dow Chemical Co., Midland, Mich., Sept 30, 1967.
(16) L. S. Hersh and O. J. Kleppa, *J. Chem. Phys.*, **42**, 1309 (1965); K. Hagemark, D. Hengstenberg, and M. Blander, *J. Chem. Eng. Data*, **17**, 216 (1972).
(17) The constant K' is essentially the same as the Sieverts' law constant, K_s, which is defined as

$$K_s = \frac{N_H}{(P_{H_2})^{1/2}} = \exp\left\{-\left[\mu_H{}^*(T, P_{H_2}) - \frac{1}{2}\mu_{H_2}{}^0(g, T, 1 \text{ atm})\right]/RT\right\}$$

where $N_H = N_{LiH}/(1 + N_{LiH})$ is the atom fraction of H in lithium. For the cases where $N_{LiH} \ll 1$, K' becomes identical with K_s.
(18) An equivalent way of defining the limiting activity coefficients is provided by eq 4 and 5. They give $\ln \gamma_2{}^* = \alpha' + (\frac{1}{2})\beta'$ and $\ln \gamma_1{}^* = \alpha'' + \beta''$.
(19) H. W. Davison, "Compilation of Thermophysical Properties of Liquid Lithium," NASA Report No. TN D-4650, 1968.
(20) The density of liquid LiH has been derived from unstated sources at six temperatures (700–950°) in F. H. Welsh, "Properties of LiH. III. Summary of GE-ANPD Data," Report No. XDC-61-5-67, 1961. These data fit the equation $d_{LiH}(g/cm^3) = 5.572 - 14.547 \times 10^{-3}T + 14.116 \times 10^{-6}T^2 - 4.593 \times 10^{-9}T^3$, where T is the Kelvin temperature.
(21) L. E. Topol, *J. Phys. Chem.*, **69**, 11 (1965).
(22) E. Veleckis, S. K. Dhar, F. A. Cafasso, and H. M. Feder, *J. Phys. Chem.*, **75**, 2832 (1971).
(23) G. M. Watson, R. B. Evans, W. R. Grimes, and N. V. Smith, *J. Chem. Eng. Data*, **7**, 285 (1962).

Metal Ion Association in Alcohol Solutions. IV. The Existence of an Inner-Sphere Complex between Erbium(III) and Perchlorate

Herbert B. Silber

Department of Chemistry, University of Maryland Baltimore County, Baltimore, Maryland 21228 *(Received June 5, 1974)*

An ultrasonic relaxation investigation of erbium(III) perchlorate solutions in aqueous methanol revealed the existence of inner-sphere perchlorate complexes below water mole fractions of 0.9. The rate constant for the formation of the inner-sphere complex at 25° is $(1.2 \pm 0.2) \times 10^8$ sec^{-1}.

The use of $LiClO_4$ or $NaClO_4$ as nonassociating "inert" electrolytes to maintain constant ionic strength in electrochemical, thermodynamic, and kinetic studies is a common technique. If an inner-sphere metal ion–perchlorate complex exists, the experimental observations can be erroneous because reactions of a solvated metal ion need not be the same as those of a metal ion–ligand complex.[1] This problem becomes more acute in solutions of lower dielectric constant than water where increased ionic association would be expected.

We have chosen to determine if an inner-sphere perchlorate complex can be detected in a test system utilizing Er(III), a lanthanide ion. There are several reasons for choosing this system. First, there exist kinetic differences in the association reactions of the lanthanides with murexide when the inert electrolyte is KNO_3 or $NaClO_4$,[2,3] and the nitrates are known to form inner-sphere complexes in aqueous solutions.[4-6] Second, kinetic studies of lanthanide complexation are starting to appear in alcohols using $NaClO_4$ as the "inert" electrolyte.[7] Third, pmr measurements have been carried out on lanthanide perchlorate systems to determine the cation solvation number, but these studies cannot detect perchlorate binding.[8,9] Fourth, we have successfully used the ultrasonic relaxation technique